Direct torque control technique for BLDC motor drive in electric vehicle applications

Sachin Chavhan[1,2], Mahesh Kumbhar[3]
[1]Shivaji University, Kolhapur, India
[2]Department of Electronics Engineering (Poly Wing), Walchand College of Engineering, Maharashtra, India
[3]Department of Electronics and Telecommunication Engineering, Rajarambapu Institute of Technology, Islampur, India

Article Info

Article history:

Received Sep 29, 2024
Revised Apr 11, 2025
Accepted May 6, 2025

Keywords:

BLDC motor
Electric vehicle
Flux
Speed
Torque

ABSTRACT

In the field of electric vehicles (EV), the hunt for the appropriate choice of motor and its control technique would be a never-ending process. The brushless DC (BLDC) motors are deployed in electric vehicles on account of higher efficiency, long life, compact size, and higher torque capacity in comparison to other types of motors. The recent advancements in power electronics have assisted in the deployment of BLDC motors in electric vehicles. These applications demand a control mechanism for the motoring mode as well as the regenerative braking mode. During the motoring mode, the power delivered to the motor is controlled, and during the regenerative braking mode, the charging of the battery takes place. Speed control strategy during motoring mode is essential to guarantee the required performance. This paper presents a direct torque control (DTC) technique for BLDC motor control for electric vehicles. The control technique and drive setup are developed to cater to the motoring mode as well as regenerative braking operation as desired for electric vehicles. MATLAB simulation and results are discussed for both modes of operation. Also, the dynamic response of the system is analyzed, which shows an average 1.1 ms response time for a 100 RPM change in speed during speeding up and 0.76 ms response time while speeding down.

Corresponding Author:

Sachin Chavhan
Department of Electronics Engineering (Poly Wing), Walchand College of Engineering
Vishrambag, Sangli 416415, Maharashtra, India
Email: sachin.chavan@walchandsangli.ac.in

1. INTRODUCTION

For electric bikes, brushless DC (BLDC) motors are preferred over other types of motors [1]. The electric bike controller deploys a BLDC motor controller. For controlling speed, different schemes have been developed over the years. These techniques include voltage control, frequency control, pulse width modulation (PWM) control, and field-oriented control. The speed control techniques often use hall sensors to get the knowledge of the angular position of the rotor for generating a PWM signal for speed control. Some recent techniques have come up with sensorless speed control [2]. Overall, these control techniques are categorized as trapezoidal and sinusoidal control. While developing the BLDC motor controller, the key blocks are sensor data acquisition, drivers, a three-phase inverter, and a control mechanism [3]. For the software part, the considerations are analogous to digital converter (ADC) sampling and conversion, PWM modules, current sensing, and battery protection circuit response [3].

A smart motor controller for an E-bike essentially takes these considerations into account, in addition to the appropriate speed control method. The control technique makes the system more efficient when regenerative braking is added [4]. For BLDC motors, torque control is significantly important as far as electric vehicles (EV) applications are concerned [5]. Apart from just speed control, a smart controller involves various physical factors such as sensors for slope, paddle assist (for electric bicycles), user interface, and many more [6], [7]. Researchers have also focused on developing fault-tolerant controllers to ensure uninterrupted EV operation [8]. More sophisticated controllers are built by using field-programmable gate array (FPGA) and advanced digital controllers [9].

The BLDC motor speed control for EV applications involves, at first, measuring the motor's actual speed. The speed measurement with hall sensors is a low-cost solution [10] for the same. The speed controller design involves modelling [11] and tuning the gains of the proportional integral derivative (PID) controller by considering BLDC motor specifications by considering the dynamic states of the motor [12]-[14].

For speed control of high-speed BLDC motors without sensors, a flux linkage function independent of speed is presented in [15], assuring a robust operation in the low-speed range and giving a correction approach for precise commutation points at the higher speeds. The robust controller [16] is developed by using a pole placement strategy and an optimal linear quadratic regulator to ensure robust stability. The spider-based controller algorithm [17] is effective in maintaining constant speed over larger intervals of time. When the hall sensor's data is clubbed with rotor speed in [18]. The ability to work independently of their correct position is made possible by the logical separation of the Hall sensors from the control transistors' switching function. It allows us to create an algorithm that can identify issues with any or all of the sensors without interfering with the motor's performance.

The switching of power electronic devices results in torque ripples. The technique of [19] reduces total harmonic distortion (THD) and torque ripples as well as improves efficiency. The DTC scheme drives the BLDC motor in a constant torque region [20]. In DTC control, the motor torque is estimated by measuring the motor voltage, and the flux is estimated by measuring the motor current. Designers and engineers have worked out with different controllers for improving the dynamic response characteristics like overshoot and rise time, with fuzzy controllers [21]. The sliding mode observer is deployed in [22] for instantaneous torque estimation. For reducing the torque ripples, the three-phase quantities of motor voltage and current are transformed into a two-axis system with the Park transformation [23], and then estimate the torque with a lookup table approach. The d-axis current is used by the sensor-less DTC technique to indirectly regulate the stator flux amplitude and directly control the torque. It is feasible to do flux-weakening operations because the stator flux is controlled. This technique [24] enables the fluctuating signals to be regulated. A straightforward look-up table for voltage vector selection is intended to provide quick torque and flux control. In field weakening regions, direct power control [25] is effective.

2. METHOD

The BLDC motor's mathematical for armature winding voltages of are expressed as (1)-(3).

$$V_a = Ri_a + L\frac{di_a}{dt} + e_a \tag{1}$$

$$V_b = Ri_b + L\frac{di_b}{dt} + e_b \tag{2}$$

$$V_c = Ri_c + L\frac{di_c}{dt} + e_c \tag{3}$$

Where ia, ib, and ic: motor current; Va, Vb, and Vc: motor's phase voltages; R=Ra=Rb=Rc: armature resistance; L=La=Lb=Lc=Ls–Lm: armature inductance; Ls: self-inductance of armature; Lm: mutual-inductance of armature; and ea, eb, and ec: motor back EMF. In matrix form (4):

$$\begin{bmatrix} V_a \\ V_b \\ V_c \end{bmatrix} = \begin{bmatrix} R+\Delta L & 0 & 0 \\ 0 & R+\Delta L & 0 \\ 0 & 0 & R+\Delta L \end{bmatrix} \begin{bmatrix} i_a \\ i_b \\ i_c \end{bmatrix} + \begin{bmatrix} e_a \\ e_b \\ e_c \end{bmatrix} \tag{4}$$

where $\Delta = \frac{d}{dt}$.

The BLDC motor's back electromotive force (EMF) is trapezoidal in nature due to permanent magnets. Hence, the back EMF is written as (5)-(7).

$$e_a = k_E \emptyset(\theta)\omega(t) \tag{5}$$

$$e_b = k_E \emptyset\left(\theta - {}^{2\pi}/_{3}\right)\omega(t) \tag{6}$$

$$e_c = k_E \emptyset\left(\theta + {}^{2\pi}/_{3}\right)\omega(t) \quad (7)$$

Where ω is the real rotor speed, KE is the back EMF constant, and θ is the angle of the rotor position. In matrix form (8):

$$\begin{bmatrix} e_a \\ e_b \\ e_c \end{bmatrix} = k\omega \begin{bmatrix} f_a(a) \\ f_b(b) \\ f_c(c) \end{bmatrix} \quad (8)$$

where ω is angular speed of the rotor; K is flux linkage; θ is actual rotor position; and $f_a(a)$, $f_b(b)$, and $f_c(c)$ are functions of the rotor angle.

The electromagnetic torque is defined as $T_e = \frac{Power}{Angular\ Frequency}$ for a three-phase BLDC motor, it can be expressed as (9).

$$T_e = \frac{e_a i_a + e_b i_b + e_c i_c}{\omega_e} \quad (9)$$

For DTC, the 3-phase AC quantities are transformed into 2-phase with Park transforms. Hence, in dq reference frame, the electromagnetic torque is expressed as (10).

$$T = \frac{3}{2}\frac{P}{\omega_e}\left[e_q i_{sq} + e_d i_{sd}\right]\theta_{re} \quad (10)$$

Where P is the number of poles; ω_e is the electrical rotor speed; e_q, e_d, i_{sq}, and i_{sd} are the dq axis back EMF and currents; and θ_{re} is the electrical rotor position.

The mathematical formulation of the BLDC motor with the DTC method is done from (1) to (10). Figure 1 shows the proposed DTC scheme for BLDC motor speed control. The system takes the input for reference speed and reference torque. On the motor side, the measurements are carried out for voltage, current, and motor speed. For speed control of the motor, the estimated torque and estimated flux are compared with the torque reference and flux reference, and generate an error signal corresponding to flux and torque. These error signals and estimated torque and flux values are used to select the switching state through a vector selection table and generate the gate control signals for the inverter.

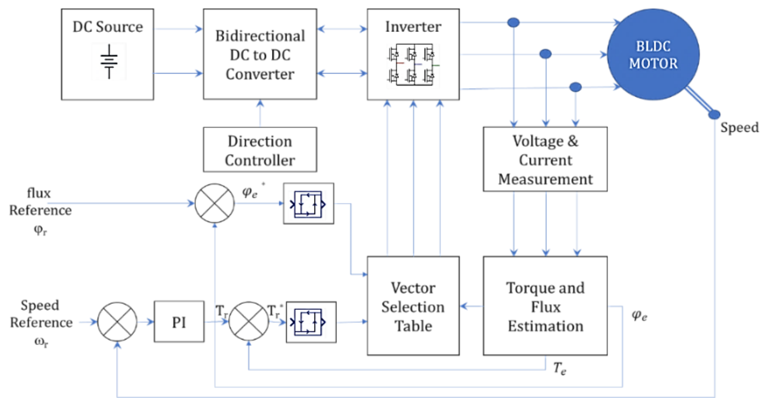

Figure 1. Block diagram of DTC control technique

3. MATLAB MODEL AND SIMULATION RESULT

The MATLAB model of the proposed BLDC motor speed controller with direct control technique is seen in Figure 2. The system consists of a bidirectional DC-DC converter and a bidirectional inverter to support power flow from the battery to the motor and vice versa. The DTC control scheme is shown in Figure 3. By measuring the motor’s voltage and current estimation of motor's torque and magnetic flux is carried out. With the integration of stator voltages, the estimated value of stator flux linkage is computed. The estimated value of stator flux and the measured value of motor current are multiplied to estimate the torque value. The control signals for the switches in the inverter bridge are then generated by comparing the estimated values of flux and torque with reference values in order to ensure that the errors in flux and torque return as quickly as possible to their accepted levels. The specifications of the selected BLDC motor and overall system are mentioned in Table 1.

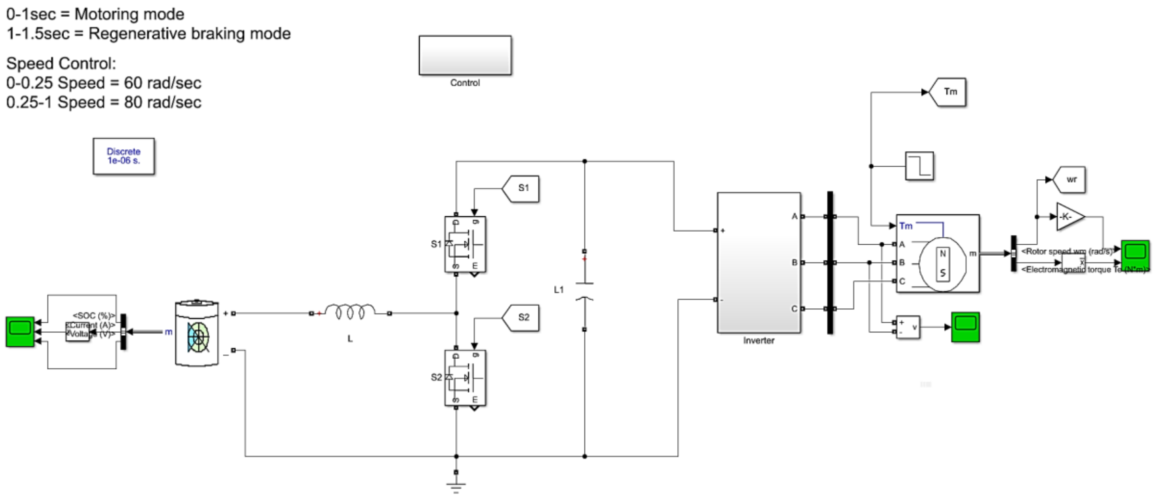

Figure 2. MATLAB model for BLDC motor control with DTC

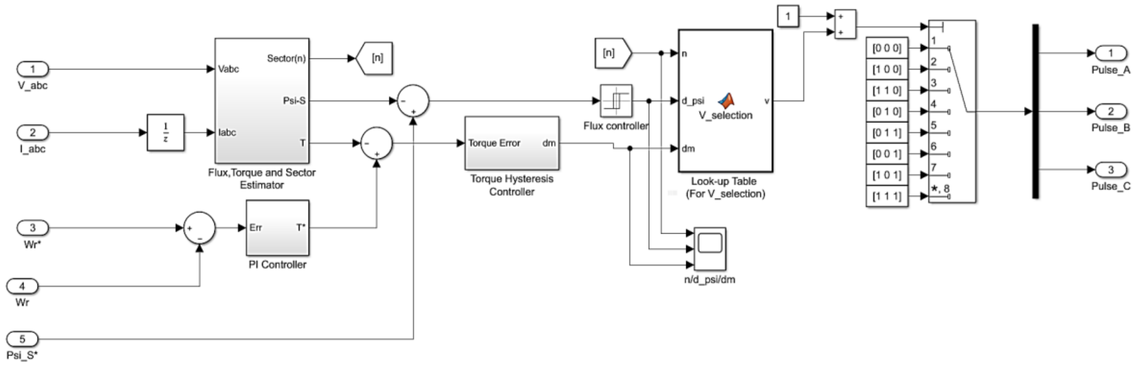

Figure 3. MATLAB model of DTC control scheme

Table 1. Specifications of the selected BLDC motor and overall system

Component	Specification
BLDC motor	Voltage: 24 V Power: 350 W RPM: 3000 No. of poles: 4
Battery	Voltage: 24 V Capacity: 18 Ah Initial SoC: 80%
Bidirectional buck-boost converter	Switching device: MOSFET Inductor: 0.1 mH
Speed control technique	Direct torque control
Inverter	MOSFET based
Controller	PI controller
Reference torque	10 Nm (during motoring mode) –10 Nm (during generation mode)
Speed change steps (RPM)	0, 100, 200, 300, 400, 500 (during motoring)

The simulation model is set to execute for period of 1.5 seconds. During this interval, the motoring mode is active between 0 to 1 second, and from 1 to 1.5 regeneration mode of operation is active. As seen in Figure 4, the torque is controlled to a constant value of 10 Nm despite speed change. The torque reversal at time instance 1 second indicates that the active power is coming out from the motor, and the BLDC motor is now acting as a generator. In the motoring mode, the speed control is active. The reference speed at start is kept at 400 RPM, and at time instance 0.5 s, its value is changed to 800 RPM. The result shows that the DTC scheme controls the actual speed to a value near to the reference speed. Also, the torque of the motor is controlled to the reference value regardless of speed. During the speed change, a notch is observed in the graph of the motor torque, which is then settled to a constant value.

The results of power flow are indicated in Figure 5 through battery state of charge (SoC). In motoring mode operation, the SoC of the battery reduces, and a gain in SoC of the battery is noted in regeneration mode. The dynamic response of the system during the change of reference speed from 400 RPM to 800 RPM is seen in Figure 6. The typical oscillation of the PI controller is seen for 3–4 cycles. The waveform of voltage across the BLDC motor stator terminals is shown in Figure 7.

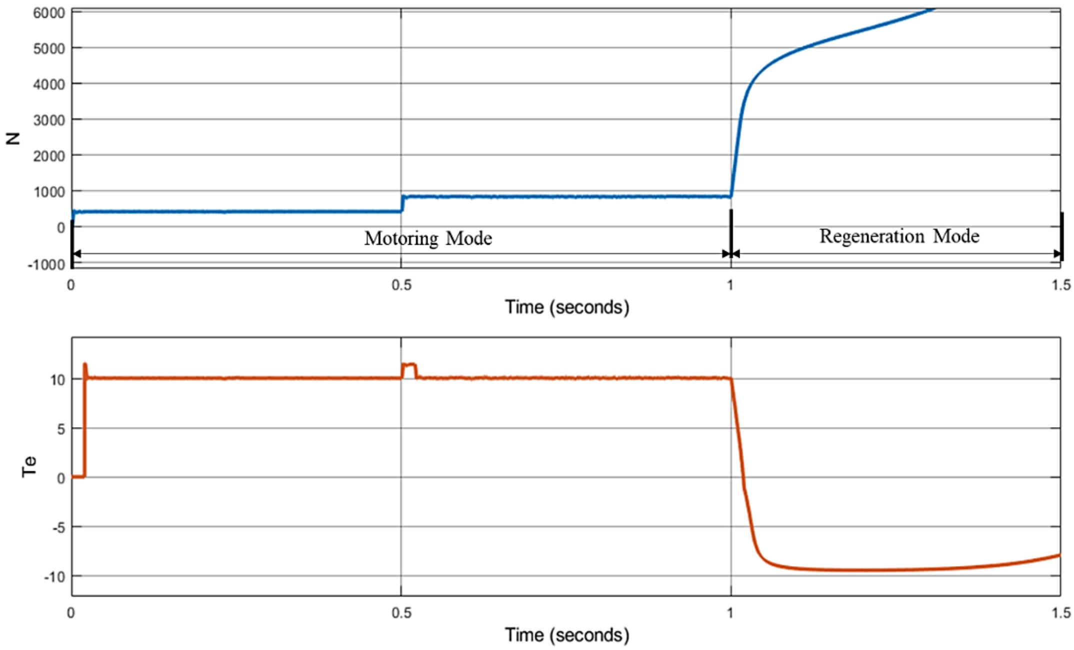

Figure 4. Speed and torque of the motor

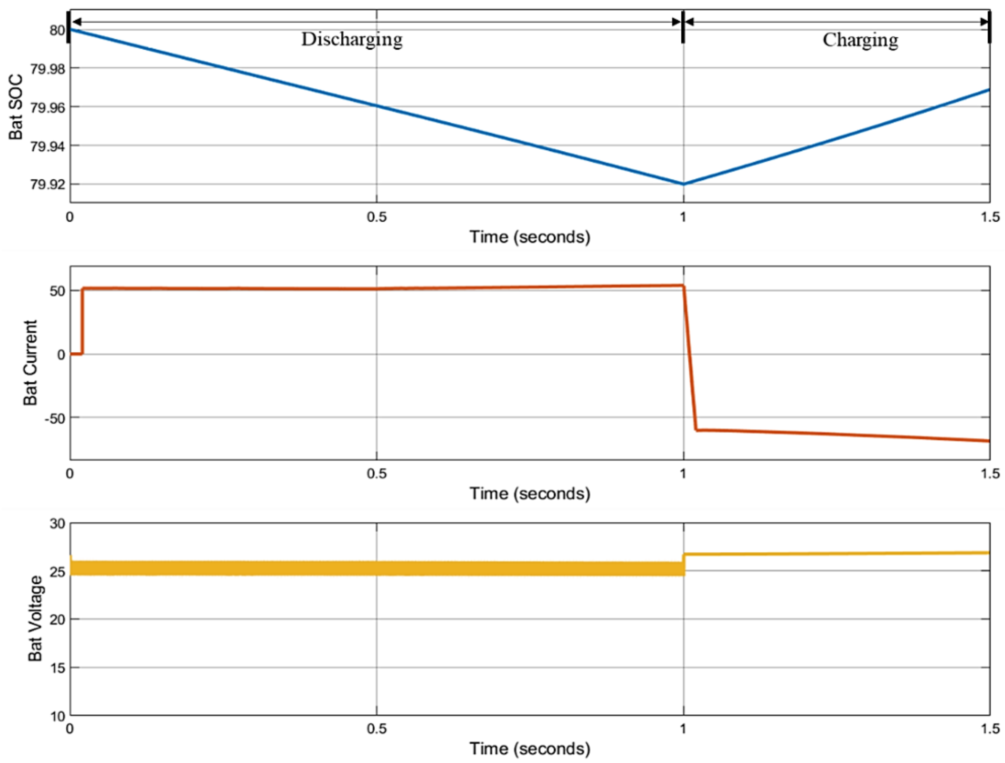

Figure 5. Battery state of the charge (SoC), voltage, and current

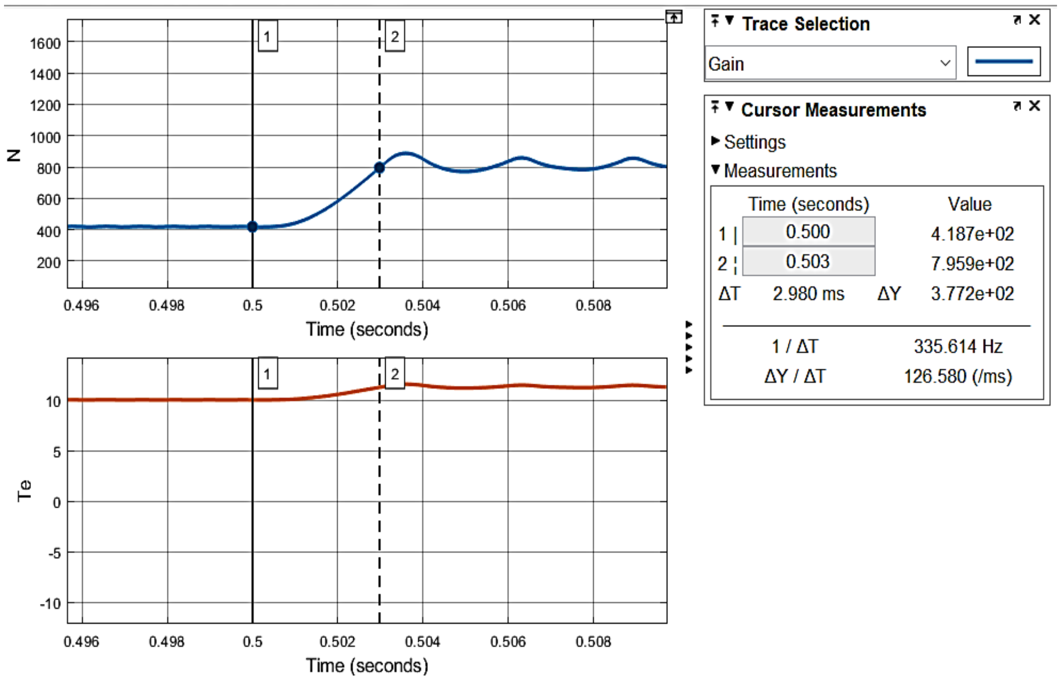

Figure 6. Dynamic response during change of reference speed

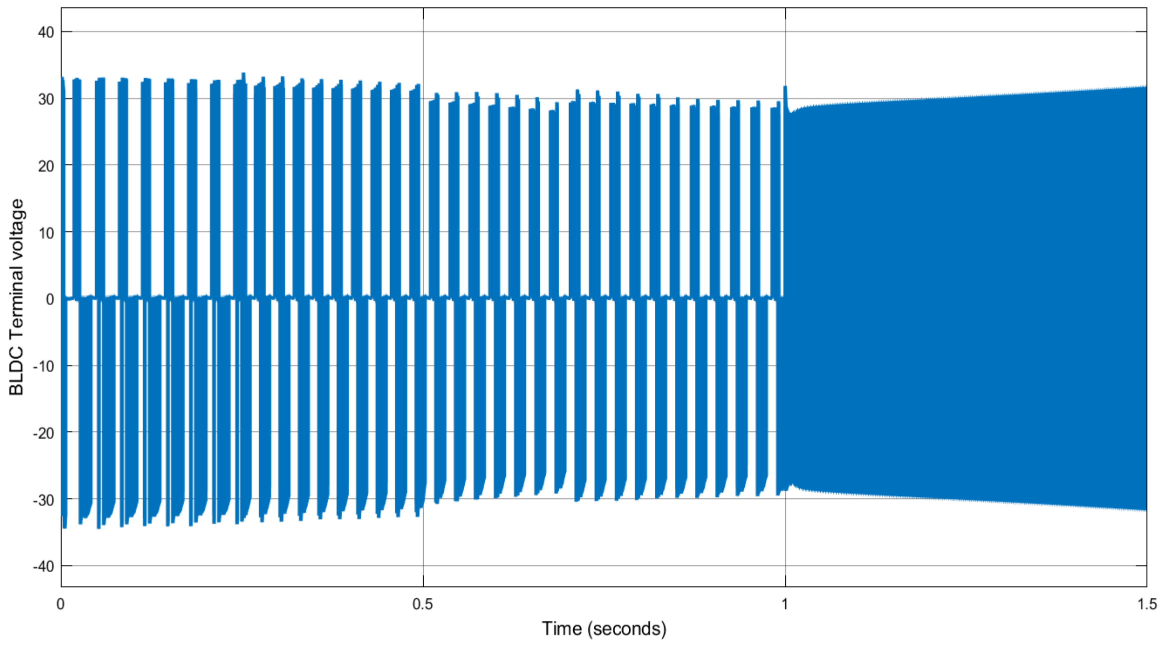

Figure 7. Voltage across the BLDC motor stator terminal

4. RESULTS AND DISCUSSION

For noting the dynamic response of the system, the model is set to execute again for a total time of 1.5 seconds. At an interval of every 0.125 seconds, the reference speed is incremented by 100 RPM up to 500 RPM. Thereafter, it is reduced to zero in the same step size. The observations of reference speed, actual speed, and time taken to reach the new speed after a step change are recorded in Table 2. The speed response of reference speed and actual speed is plotted as seen in Figure 8. The zoomed view of the same is shown in Figures 9(a)-9(d) (see Appendix). The average rise time of 1.1 ms is noted for every 100 RPM change in speed during an increase in speed. During a decrease in speed change, the average fall time is noted to be

0.76 ms. The significant undershoots are seen during a decrease in the speed of the motor as compared to the overshoots observed during an increase in the speed of the motor.

Table 2. Result summary of dynamic response

Previous reference speed (RPM)	New reference speed (RPM)	Actual speed (RPM)	Rise/fall time (ms) (time taken to reach new reference speed)
0	100	100	1.01
100	200	200	1.21
200	300	300	1.17
300	400	400	1.20
400	500	500	1.18
500	400	400	0.72
400	300	300	0.77
300	200	200	0.76
200	100	100	0.78
100	0	0	0.76

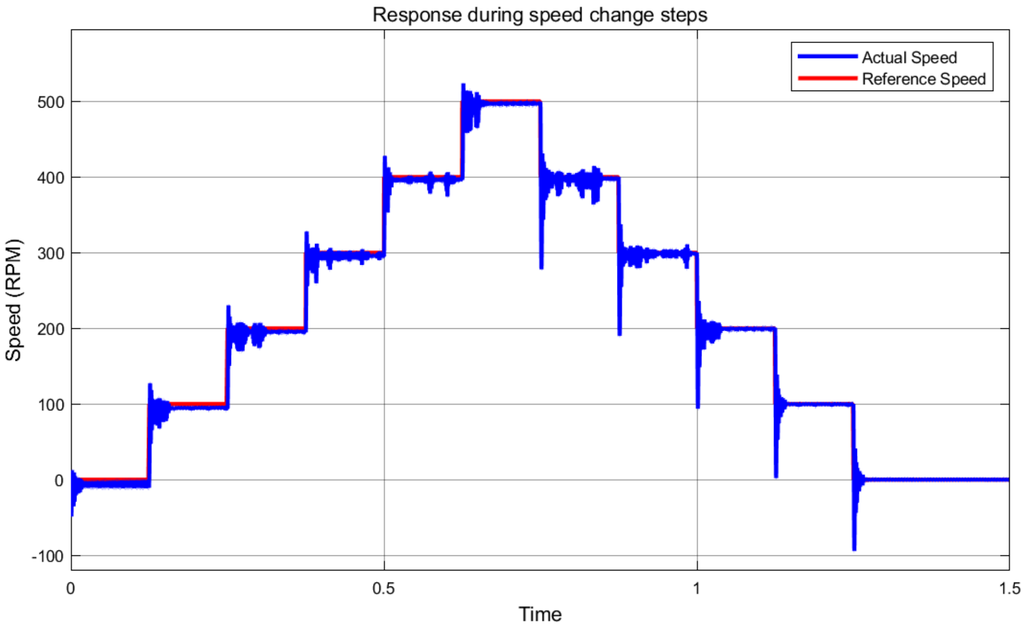

Figure 8. Dynamic response of the system during speeding up and down

5. CONCLUSION

This paper discusses DTC-based BLDC motor speed control. The switching signals for DTC are generated with the help of a look-up table, which confines the torque error within the specified hysteresis band. This is done with the help of the rotor flux vector position and torque error. Despite a notch during speed change, the torque obtained in DTC control is constant. The developed system is seen to be effective in tracking the actual speed near to the reference speed. The dynamic response is also analyzed, which shows the rise time of 1.1 ms per 100 RPM increase in speed and average fall time of 0.76 ms during a decrease in speed by 100 RPM. The oscillations in speed are observed particularly during speed drops due to the inertia effect and the load on the motor.

FUNDING INFORMATION

The work presented in this paper has not received funding from any public private or non-profit agency.

AUTHOR CONTRIBUTIONS STATEMENT

This journal uses the Contributor Roles Taxonomy (CRediT) to recognize individual author contributions, reduce authorship disputes, and facilitate collaboration.

Name of Author	C	M	So	Va	Fo	I	R	D	O	E	Vi	Su	P	Fu
Sachin Chavhan	✓	✓	✓	✓	✓	✓	✓	✓	✓	✓	✓		✓	
Mahesh Kumbhar		✓		✓	✓					✓	✓	✓		

C : **C**onceptualization
M : **M**ethodology
So : **So**ftware
Va : **Va**lidation
Fo : **Fo**rmal analysis
I : **I**nvestigation
R : **R**esources
D : **D**ata Curation
O : Writing - **O**riginal Draft
E : Writing - Review & **E**diting
Vi : **Vi**sualization
Su : **Su**pervision
P : **P**roject administration
Fu : **Fu**nding acquisition

CONFLICT OF INTEREST STATEMENT

The authors affirm that they have no known financial or interpersonal conflicts that would have appeared to have an impact on the findings presented in this paper. Authors state no conflict of interest.

DATA AVAILABILITY

The authors confirm that the experimental data supporting the conclusions of this research are provided within the article.

REFERENCES

[1] S. Krishnamoorthy and P. P. K. Panikkar, "A comprehensive review of different electric motors for electric vehicles application," *International Journal of Power Electronics and Drive Systems*, vol. 15, no. 1, pp. 74–90, 2024, doi: 10.11591/ijpeds.v15.i1.pp74-90.

[2] J. Cheng, C. Lu, G. Zhang, C. Wu, and Y. Huang, "Research and design of electric vehicle controller based on brushless DC motor," in *2017 36th Chinese Control Conference (CCC)*, 2017, pp. 10132–10136, doi: 10.23919/ChiCC.2017.8028971.

[3] D. Mohanraj *et al.*, "A review of BLDC motor: state of art, advanced control techniques, and applications," *IEEE Access*, vol. 10, pp. 54833–54869, 2022, doi: 10.1109/ACCESS.2022.3175011.

[4] Z. Zhang, J. Shen, and B. Li, "Design of controller in electric bicycle," *Journal of Modern Applied Science*, vol. 5, no. 5, pp. 125–130, 2011, doi: 10.5539/mas.v5n5p125.

[5] B. V. Narayana, C. Govinda, V. Srinivasa Rao, R. P. S. D. Bhima, J. Pavan, and N. Rajesh, "Improved execution of the BLDC motor using 3- phase conduction mode for electric vehicle," in *2021 5th International Conference on Computing Methodologies and Communication (ICCMC)*, Apr. 2021, pp. 624–628, doi: 10.1109/ICCMC51019.2021.9418284.

[6] O. Trescases, S. O'Loughlin, and W. T. Ng, "A smart motor controller for E-bike applications," *Industry*, vol. 43, no. 37, pp. 16–19, 2003.

[7] K. F. I. Faruque, N. Nawshin, M. F. Bhuiyan, M. R. Uddin, M. Hasan, and K. M. Salim, "Design and development of BLDC controller and its implementation on E-bike," in *2018 International Conference on Recent Innovations in Electrical, Electronics and Communication Engineering, ICRIEECE 2018*, 2018, pp. 1461–1465, doi: 10.1109/ICRIEECE44171.2018.9008597.

[8] G. Sajitha, N. Mayadevi, V. P. Mini, and R. Harikumar, "Fault-tolerant control of BLDC motor drive for electric vehicle applications," in *2019 International Conference on Power Electronics Applications and Technology in Present Energy Scenario (PETPES)*, Aug. 2019, pp. 1–6, doi: 10.1109/PETPES47060.2019.9003925.

[9] R. M. Pindoriya, S. Rajendran, and P. J. Chauhan, "Field programmable gate array based speed control of BLDC motor," in *2015 IEEE Innovative Smart Grid Technologies - Asia (ISGT ASIA)*, Nov. 2015, pp. 1–6, doi: 10.1109/ISGT-Asia.2015.7387048.

[10] V. Naveen and T. B. Isha, "A low cost speed estimation technique for closed loop control of BLDC motor drive," in *2017 International Conference on Circuit, Power and Computing Technologies (ICCPCT)*, 2017, doi: 10.1109/ICCPCT.2017.8074312.

[11] P. Suganthi, S. Nagapavithra, and S. Umamaheswari, "Modeling and simulation of closed loop speed control for BLDC motor," in *2017 Conference on Emerging Devices and Smart Systems, (ICEDSS)*, 2017, pp. 229–233, doi: 10.1109/ICEDSS.2017.8073686.

[12] H. Sarma and A. Bardalai, "An intelligent PID controller tuning for speed control of BLDC motor using driving training-based optimization," *International Journal of Power Electronics and Drive Systems (IJPEDS)*, vol. 14, no. 4, pp. 2474–2486, 2023, doi: 10.11591/ijpeds.v14.i4.pp2474-2486.

[13] E. Anitha and P. Vairaprakash, "Design of dynamic states and digital speed control of BLDC motor," in *2016 International Conference on Circuit, Power and Computing Technologies (ICCPCT)*, 2016, doi: 10.1109/ICCPCT.2016.7530313.

[14] B. Bairwa, M. Murari, M. Shahapur, K. M. R, and M. F. Khan, "Speed control of BLDC motor using PI controller," in *2023 International Conference for Advancement in Technology (ICONAT)*, Jan. 2023, pp. 1–6, doi: 10.1109/ICONAT57137.2023.10080074.

[15] S. Chen, G. Liu, and L. Zhu, "Sensorless control strategy of a 315 kW high-speed BLDC motor based on a speed-independent flux linkage function," *IEEE Transactions on Industrial Electronics*, vol. 64, no. 11, pp. 8607–8617, Nov. 2017, doi: 10.1109/TIE.2017.2698373.

[16] P. M. de Almeida, R. L. Valle, P. G. Barbosa, V. F. Montagner, V. Cuk, and P. F. Ribeiro, "Robust control of a variable-speed BLDC motor drive," *IEEE Journal of Emerging and Selected Topics in Industrial Electronics*, vol. 2, no. 1, pp. 32–41, Jan. 2021, doi: 10.1109/JESTIE.2020.3035055.

[17] M. P. Maharajan and S. A. E. Xavier, "Design of speed control and reduction of torque ripple factor in BLDC motor using spider based controller," *IEEE Transactions on Power Electronics*, vol. 34, no. 8, pp. 7826–7837, Aug. 2019, doi: 10.1109/TPEL.2018.2880916.

[18] K. Kolano, "Improved sensor control method for BLDC motors," *IEEE Access*, vol. 7, pp. 186158–186166, 2019, doi: 10.1109/ACCESS.2019.2960580.

[19] H. K. S. Ransara and U. K. Madawala, "A torque ripple compensation technique for a low-cost brushless DC motor drive," *IEEE Transactions on Industrial Electronics*, vol. 62, no. 10, pp. 6171–6182, Oct. 2015, doi: 10.1109/TIE.2015.2423664.
[20] S. B. Ozturk and H. A. Toliyat, "Direct torque control of brushless DC motor with non-sinusoidal back-EMF," in *2007 IEEE International Electric Machines & Drives Conference*, May 2007, pp. 165–171, doi: 10.1109/IEMDC.2007.383571.
[21] N. Parhizkar, M. Shafiei, and M. B. Kouhshahi, "Direct torque control of brushless DC motor drives with reduced starting current using fuzzy logic controller," in *2011 International Conference on Uncertainty Reasoning and Knowledge Engineering*, Aug. 2011, pp. 129–132, doi: 10.1109/URKE.2011.6007863.
[22] Y. Liu, Z. Q. Zhu, and D. Howe, "Instantaneous torque estimation in sensorless direct torque controlled brushless DC motors," in *Fourtieth IAS Annual Meeting. Conference Record of the 2005 Industry Applications Conference, 2005*, vol. 3, pp. 2140–2146, doi: 10.1109/IAS.2005.1518743.
[23] T. R. Sharma and Y. Pal, "Direct torque control of BLDC drives with reduced torque pulsations," in *2019 3rd International conference on Electronics, Communication and Aerospace Technology (ICECA)*, Jun. 2019, pp. 1242–1247, doi: 10.1109/ICECA.2019.8822141.
[24] R. Heidari, G. A. Markadeh, and S. Abazari, "Direct torque and indirect flux control of brushless DC motor with non-sinusoidal back-EMF without position sensor," in *2011 19th Iranian Conference on Electrical Engineering, ICEE 2011*, 2011.
[25] H. Masoudi, A. Kiyoumarsi, S. M. Madani and M. Ataei, "Closed-loop direct power control of brushless DC motor in field weakening region," in *IEEE Transactions on Transportation Electrification*, vol. 10, no. 2, pp. 3482-3491, Jun. 2024, doi: 10.1109/TTE.2023.3305050.

APPENDIX

(a)

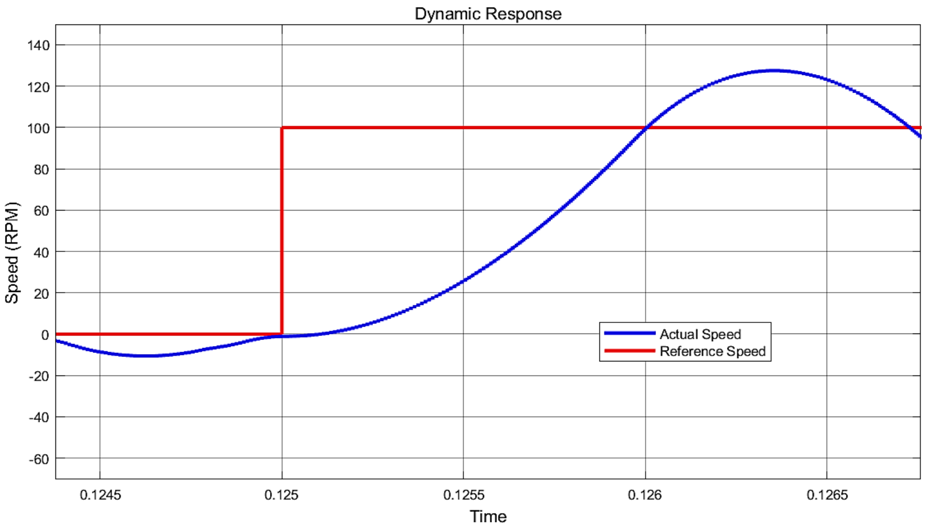

(b)

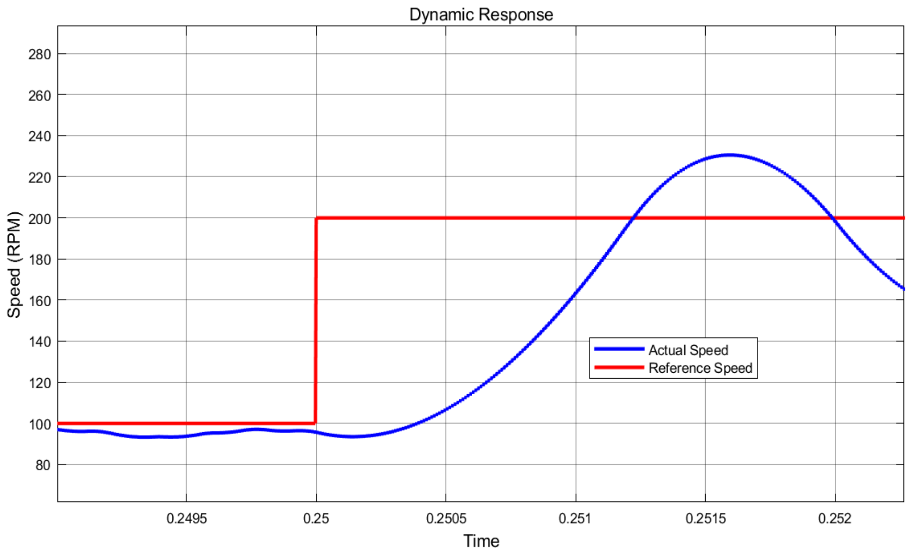

Figure 9. Zoomed view of dynamic response of the system during speed changes: (a) speed change from 0 to 100 RPM and (b) speed change from 100 to 200 RPM

(c)
(d)

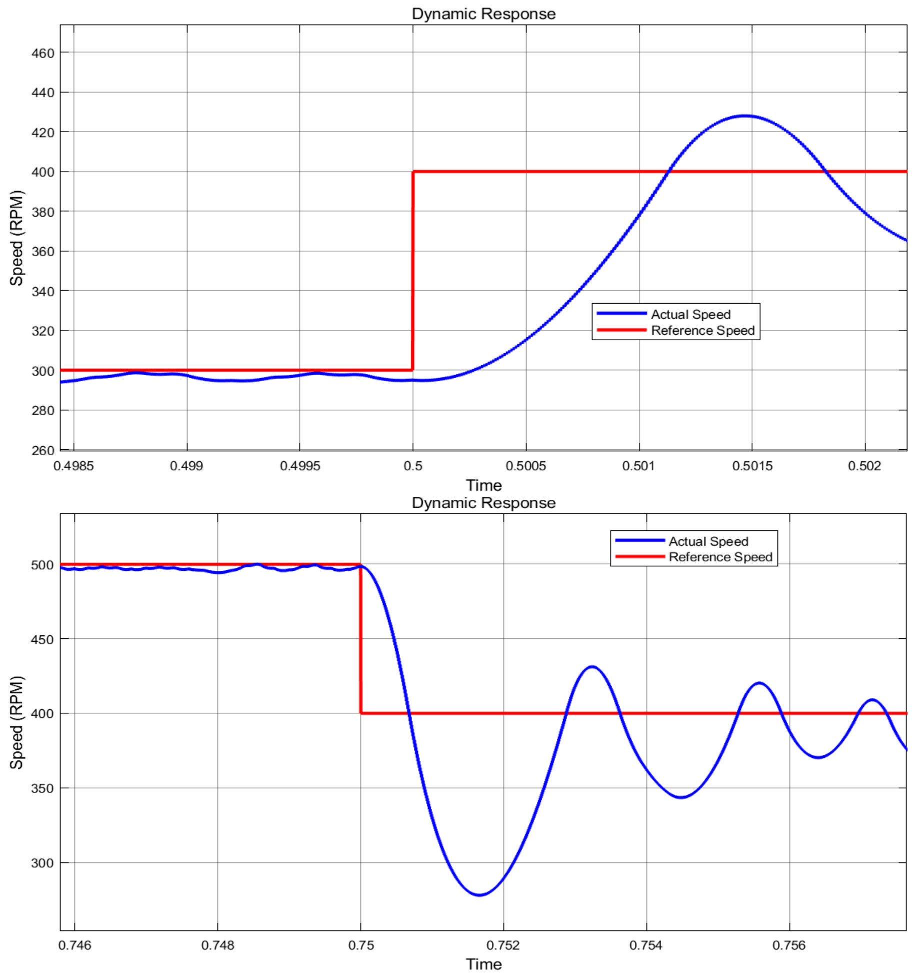

Figure 9. Zoomed view of dynamic response of the system during speed changes: (c) speed change from 300 to 400 RPM and (d) speed change from 400 to 300 RPM (continued)

BIOGRAPHIES OF AUTHORS

Sachin Chavhan is a lecturer in the Department of Electronics Engineering (Poly Wing) at the Walchand College of Engineering, Sangli, Maharashtra, India. He received his B.E. and M.E. degrees in Electronics and Telecommunication Engineering from the University of Pune and North Maharashtra University, Jalgaon, India, in 2010 and 2013, respectively. He is currently pursuing his Ph.D. at Shivaji University, Kolhapur. He has 10 years of experience. His research interests include power electronics, motor drives, embedded and VLSI systems, artificial intelligence, and optimization techniques. He can be contacted at email: sachin.chavan@walchandsangli.ac.in or sachin.chavhan22@gmail.com.

Mahesh Kumbhar is an Associate Professor in Department of Electronics and Telecommunication Engineering, at Rajarambapu Institute of Technology, Islampur, India since 1997; and he received the B.E. and M.E. degrees in Electronics Engineering from Shivaji University, Maharashtra, India in 1994 and 2005, respectively; and Ph.D. degree in Electronics Engineering from Shivaji University Kolhapur in 2015. His research interests include the field of power electronics, machine learning, artificial intelligence, and WSN applications. He can be contacted at email: mahesh.kumbhar@ritindia.edu.